Theor Chim Acta (1994) 89: 415–427

Theoretica Chimica Acta

© Springer-Verlag 1994

A novel finite element method implementation for calculating bound states of triatomic systems: Application to the water molecule

J. J. Soares Neto*, F. V. Prudente
Departamento de Física, Universidade de Brasília, 70.910-900 Brasília-DF, Brazil

Received March 25, 1994/Final revision received July 19, 1994/Accepted August 30, 1994

Summary. The p-version of the finite element method is utilized in a fully three-dimensional bound state calculation of the vibrational spectrum of H_2O. The algorithm shows the possibility of using the finite element method to calculate highly excited vibrational levels of triatomic molecules.

Key words: Hyperspherical coordinates – Ro-vibrational states

1. Introduction

The recent effort to construct algorithms for calculating accurate ro-vibrational states of triatomic molecules has led to the development of efficient numerical procedures. The discrete variable representation and the successive diagonalization and truncation technique developed by Light's group has already been applied to many systems and, among them, we cite LiCN/LiNC [1, 2], HCN/HNC [3–6] and van der Waals complexes [7]. Tennyson and collaborators [8–10] developed algorithms based on Jacobi coordinates and converged highly excited vibrational levels of H_3^+. Carter and Meyer [11] and Bačić and Zhang [12, 13] also developed techniques for calculating high lying states of D_{3h} molecules and applied the program to H_3^+. The water molecule has also been studied utilizing fully three-dimensional methods. A calculation by Bačić et al. [14] utilized a Sorbie–Murrel-type potential energy surface [15] and obtained a spectrum which is not in good agreement with the experimental measurements. The discrepancy is probably due to the potential energy surface. Soares Neto and Linderberg [16], in a first attempt to use the finite element method for bound state problems, developed an algorithm based on the h-version of the finite element method and applied it to the study of H_2O using a potential energy surface fitted by Jensen [17].

More recently, several calculations for the ro-vibrational energies of water have appeared in the literature which give results for highly excited ro-vibrational levels which are in good agreement with experimental measurements. Fernley et al. [18]

* *Present address*: California Institute of Technology, Division of Chemistry and Chemical Engineering, Noyes Laboratory of Chemical Physics, Pasadena, 91125, USA

applied Radau coordinates and the discrete variable representation to calculate states up to 22000 cm^{-1} with four potential energy surfaces. They concluded that Jensen's potential [17] reproduces the observed energies well but shows a small systematic error for many higher band origins. Wei and Carrington [19] and Choi and Light [20] studied high lying vibrational levels of the water molecule applying a discrete variable representation. Choi and Light [20] also investigated local/normal mode transitions, Fermi resonances, Darling–Dennison interactions and the modes separabilities. We also cite a recent work by Tennyson [21] where he calculates rotationally excited states of H_2S, H_2O and H_3^+.

The wave function of a molecule in a high lying vibrational state may be spread over a large region of the nuclear configuration space. Moreover, the wave function is highly oscillatory and a procedure to calculate it must be able to describe the system accurately in the whole region. This imposes serious difficulties and the more traditional methods [22] are accurate for the lower levels but fail for the higher ones.

The solution of the Schrödinger equation for vibrational states of a triatomic molecule involves the choice of good coordinates and a numerical method for expanding the wave function. Moreover, the matrix associated with the problem tends to be large and contraction procedures must generally be used in order to make the problem feasible within the computational resources at hand.

The hyperspherical coordinates are now of common use in both scattering [23–27] and bound states [28–30] calculations. The triatomic system, expressed in the center of mass coordinate system, may be described by a hyperradius, which ranges from zero to infinity, and a set of five hyperangles that have finite ranges. The six hyperspherical coordinates may be divided into two sets. The potential energy surface depends on three internal coordinates and the tumbling and rotation of the system is described by the three remaining ones. There are different ways of defining a set of hyperspherical coordinates but all definitions are simply related to each other. The set we use in this paper was developed by Mead [31] and intensively utilized by Linderberg and collaborators [32–35].

The finite element method is a variational numerical approach frequently applied in engineering problems [36–37]. Its utilization in theoretical chemistry is, however, not extensive. The finite element method is a general name for several procedures which uses the discretization of the space in elements and the expansion of the wave function in terms of polynomials for each of these elements. There are two versions of the finite element method. In the h-version one expands the wave function in all elements with polynomials of the same degree [38]. The convergence, in this case, is achieved when the number of elements becomes big enough. The p-version allows one to use different degrees of polynomials in different elements [39, 40]. In this way, one can place high degree polynomials where the potential allows the wave function to have amplitude and low degree polynomials where the wave function has negligible amplitude. Convergence can be reached by balancing the number of elements in the mesh and the degree of the polynomials in each element.

In the present work a new algorithm utilizing the p-version of the finite element method and the hyperspherical coordinates is used. The finite element method produces large matrices, which are, however, symmetric and sparse. The problem matrix becomes too large when we need to calculate many vibrational states. A procedure to contract the matrix is necessary and we develop a method, based upon the successive diagonalization and truncation procedure, adapted to the finite element method. The potential energy surface is the same as applied in the

previous calculation [17]. We calculated vibrational states to even symmetry up to 16000 cm^{-1} and of odd symmetry up to 13000 cm^{-1}. The limitation is due to the computer facilities available at the Department of Physics, University of Brasilia (VAX-8350). The algorithm would be able to converge more states on a more powerful machine.

The paper is organized as follows. In Section 2 we discuss the hyperspherical coordinates. Section 3 describes the one and two-dimensional theory of the p-version of the finite element method. Section 4 shows the implementation details and in Section 5 our results are discussed and compared to the experimental measurements. Finally, in Section 6 we give our concluding remarks.

2. Hyperspherical coordinates

The hyperspherical coordinates were introduced by nuclear physicists aiming at studying few body problems [41–44]. The introduction of such a system of coordinates in quantum chemistry was done by Kuppermann [45] and Johnson [46, 47]. The hyperspherical coordinates have successfully been applied to scattering [23–27] and bound state [28–30] calculations involving triatomic molecules. We give here basic definitions and refer the reader to the references cited above for more details.

We first introduce the mass weighted Jacobi coordinates,

$$\boldsymbol{G} = \frac{(m_1\boldsymbol{X}_1 + m_2\boldsymbol{X}_2 + m_3\boldsymbol{X}_3)}{M}, \tag{1}$$

$$\boldsymbol{R} = \frac{1}{M}\left(\frac{m_1}{m_1 + m_3}\right)^{1/2} \cdot [m_1(\boldsymbol{X}_1 - \boldsymbol{X}_2) + m_3(\boldsymbol{X}_1 - \boldsymbol{X}_3)], \tag{2}$$

$$\boldsymbol{r} = \left[\frac{m_2 m_3}{M(m_2 + m_3)}\right]^{1/2} \cdot (\boldsymbol{X}_2 - \boldsymbol{X}_3). \tag{3}$$

The vector $\boldsymbol{G}$ is the center of mass of the system; m_1, m_2 and m_3 are the masses of the three nuclei and M is the total mass. The vectors $\boldsymbol{X}_i$, $i = 1, 2, 3$, give the position of each nucleus in relation to the laboratory system.

The internal hyperspherical coordinates are defined as

$$q = (\boldsymbol{R}\cdot\boldsymbol{R} + \boldsymbol{r}\cdot\boldsymbol{r})^{1/2}, \tag{4}$$

$$\rho = \frac{[(\boldsymbol{R}\cdot\boldsymbol{R} - \boldsymbol{r}\cdot\boldsymbol{r})^2 + 4(\boldsymbol{R}\cdot\boldsymbol{r})^2]}{(\boldsymbol{R}\cdot\boldsymbol{R} + \boldsymbol{r}\cdot\boldsymbol{r})^2}, \tag{5}$$

$$\theta = \operatorname{arctg}\left(\frac{2\boldsymbol{R}\cdot\boldsymbol{r}}{\boldsymbol{R}\cdot\boldsymbol{R} - \boldsymbol{r}\cdot\boldsymbol{r}}\right). \tag{6}$$

The quantity q, the hyperradius, has a range varying from zero to infinity. The hyperangles ρ and θ are defined in the range $\rho = [0, 1]$ and $\theta = [0, 2\pi]$. The potential energy surface of a triatomic molecule, written in terms of hyperspherical coordinates, depends upon q, ρ and θ. The Schrödinger equation in this set of

hyperspherical coordinate for the total angular momentum $J = 0$ is given by

$$\left\{ -\frac{1}{2M}\left[\frac{\partial^2}{\partial q^2} + \frac{4}{q^2}\frac{\partial}{\partial \rho}(1-\rho^2)\frac{\partial}{\partial \rho} + \frac{4}{q^2\rho^2}\frac{4}{q^2\rho^2}\frac{\partial^2}{\partial \theta^2}\right] + W(q,\rho,\theta) + \frac{15}{8Mq^2}\right\} \Psi(q,\rho,\theta) = E\Psi(q,\rho,\theta). \tag{7}$$

The function $W(q, \rho, \theta)$ is the potential energy surface. We expand the wave function $\Psi(q, \rho, \theta)$ as follows:

$$\Psi(q,\rho,\theta) = \sum_{ik} Q_i(q)\Omega_k(\rho,\theta)a_{ik}. \tag{8}$$

In the following section we will develop the one- and two-dimensional theory of the p-version of the finite element method and use it to express the functions $Q_i(q)$ and $\Omega_k(\rho, \theta)$.

3. The p-version of the finite element method

Calculations have been performed for molecular problems using the finite element method. Jaquet [48, 49] applied a two-dimensional approach to calculate the cross section for the reactive scattering between an atom and a diatomic molecule. Sato and Iwata [50] also used two-dimensional finite element method to deal with bound state problems. Fully three-dimensional calculations have been reported by Kuppermann and Hipes [51], Parker et al. [52] and Linderberg and collaborators [53–55]. We also mention applications of the finite element method to calculate the electronic structure of atoms and molecules [56–60]. Most of the published work applies the h-version of the finite element method. Clementi and collaborators [60] applied the one-dimensional p-version to electronic structure calculations.

One-dimensional theory

The finite element method basically uses two steps for expanding the wave function. The space is discretized into elements and the wave function is represented, within each element, by polynomials. The p-version uses the so-called interpolation and shape functions. If we consider an element $\overline{AB}$, the interpolation functions $I_1(q)$ and $I_2(q)$ are first degree polynomials defined as

$$I_1(q) = \frac{B-q}{B-A} \tag{9}$$

and

$$I_2(q) = \frac{q-A}{B-A}. \tag{10}$$

The function $I_1(q)$ has amplitude one at point A and zero at B and $I_2(q)$ is one at B and zero at A. The shape functions are defined as linear combinations of Legendre polynomials and have the important feature of being zero at both points

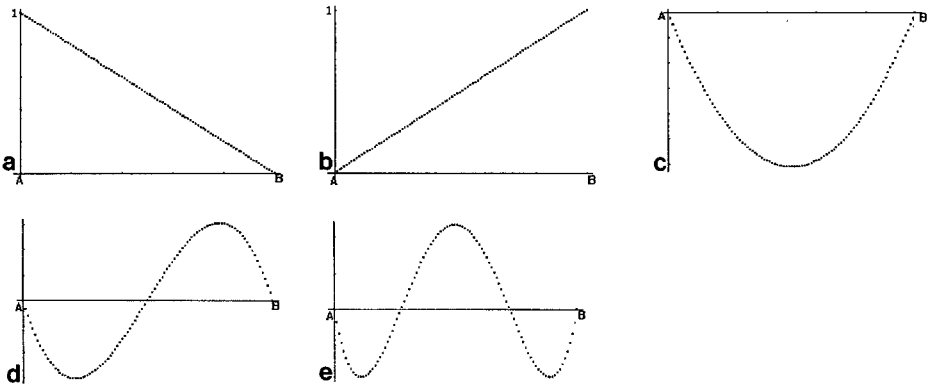

Fig. 1a–e. The one-dimensional interpolation and shape functions of the finite element method p-version. The shape functions have null amplitude at the two edges of the element; **a** interpolation function $I_1(q)$; **b** interpolation function $I_2(q)$; **c** shape function $S_1(q)$; **d** shape function $S_2(q)$; **e** shape function $S_3(q)$

A and B. They are written as

$$S_n(q) = \frac{1}{(4n+2)^{1/2}} [P_{n+1}(y) + P_{n-1}(y)], \tag{11}$$

where the functions $P_n(y)$ are the Legendre polynomials and $y = 2I_1(q) - 1$. Figure 1 shows the interpolation functions $I_1(q)$ and $I_2(q)$ as well as the shape functions $S_1(q)$, $S_2(q)$ and $S_3(q)$.

A function $f(q)$ may be expanded in terms of $I_1(q)$, $I_2(q)$ and $S_n(q)$, $n = 1, 2, \ldots, N$, as follows:

$$f(q) = \sum_{n=1}^{2} I_n(q) a_n + \sum_{n=1}^{N} S_n(q) b_n . \tag{12}$$

In the finite element theory the expansion coefficients a_n and b_n are variational parameters.

Two-dimensional theory

A two-dimensional region may be discretized by triangles and we consider the element ABC of the mesh. It is convenient to define the baricentric coordinates $a(\rho, \theta)$, $b(\rho, \theta)$ and $c(\rho, \theta)$,

$$a(\rho, \theta) = \frac{\begin{vmatrix} 1 & 1 & 1 \\ \theta & \theta_b & \theta_c \\ \rho & \rho_b & \rho_c \end{vmatrix}}{\begin{vmatrix} 1 & 1 & 1 \\ \theta_a & \theta_b & \theta_c \\ \rho_a & \rho_b & \rho_c \end{vmatrix}}, \tag{13}$$

$$b(\rho,\theta)=\frac{\begin{vmatrix}1 & 1 & 1\\ \theta_a & \theta & \theta_c\\ \rho_a & \rho & \rho_c\end{vmatrix}}{\begin{vmatrix}1 & 1 & 1\\ \theta_a & \theta_b & \theta_c\\ \rho_a & \rho_b & \rho_c\end{vmatrix}}, \tag{14}$$

$$c(\rho,\theta)=\frac{\begin{vmatrix}1 & 1 & 1\\ \theta_a & \theta_b & \theta\\ \rho_a & \rho_b & \rho\end{vmatrix}}{\begin{vmatrix}1 & 1 & 1\\ \theta_a & \theta_b & \theta_c\\ \rho_a & \rho_b & \rho_c\end{vmatrix}}. \tag{15}$$

The baricentric coordinates are first degree polynomials where $a(\rho,\theta)$ has amplitude one at vertex A and zero at the line $\overline{BC}$. The other coordinates, $b(\rho,\theta)$ and $c(\rho,\theta)$, have the same property in relation to the vertices B and C, respectively. The two-dimensional baricentric coordinates play the role of the interpolation functions in the one-dimensional finite element method theory.

We may compose higher degree polynomials applying a strategy similar to the one in the one-dimensional case. We have two kinds of two-dimensional shape functions. The first one has amplitude along one edge of the triangle and null amplitude along the two other sides. They may be constructed as follows:

$$D_j^{\overline{AC}}(\rho,\theta)=a(\rho,\theta)*S_j[2c(\rho,\theta)-1], \tag{16}$$

where $S_j[2c(\rho,\theta)-1]$ is a one-dimensional shape function written as

$$S_j[2a(\rho,\theta)-1]=\frac{1}{(4j+2)^{1/2}}\{P_{j+1}[2a(\rho,\theta)-1]+P_{j-1}[2a(\rho,\theta)-1]\}.$$

We verify that the argument $2a(\rho,\theta)-1$ is between -1 and 1 for any value of ρ and θ within the triangle ABC. The function $D_j^{\overline{AC}}(\rho,\theta)$ has amplitude different from zero along the line $\overline{AC}$. The functions $D_j^{\overline{AC}}(\rho,\theta)$ and $D_j^{\overline{BC}}(\rho,\theta)$ may be constructed in a similar way. Figure 2 shows the behavior of the baricentric coordinate $a(\rho,\theta)$ as well as of some shape functions The other kind of shape functions vanish at all edges of the triangle ABC and they are called bubble functions. They are built in the following way:

$$V_{ijk}(\rho,\theta)=S_i[2a(\rho,\theta)-1]*S_j[2b(\rho,\theta)-1]*S_k[2c(\rho,\theta)-1]. \tag{17}$$

The fact that the amplitude of both kinds of two-dimensional shape functions vanishes at all vertices of the triangle allows one to place different number of such functions in different elements of the mesh [60].

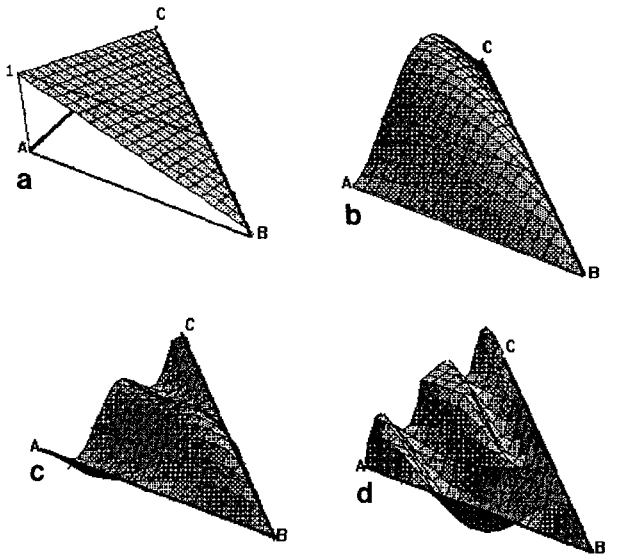

Fig. 2a–d. The finite element method functions utilized to expand the hyperangular space. We show the baricentric coordinate $a(\rho, \theta)$ and the shape functions $D_j^{\overline{AC}}(\rho, \theta)$ which have amplitude along the edge $\overline{AC}$; **a** The baricentric coordinate $a(\rho, \theta)$; **b** the shape function $D_1^{\overline{AC}}(\rho, \theta)$; **c** the shape function $D_2^{\overline{AC}}(\rho, \theta)$; **d** the shape function $D_3^{\overline{AC}}(\rho, \theta)$

4. Implementation details

The finite element method is a variational theory and we define a functional as follows,

$$J = \sum_{i,i'} \sum_{k,k'} \left\{ \int \mathrm{d}q\, \rho \mathrm{d}\rho\, \mathrm{d}\theta\, a_{ik}^* Q_i^*(q) \Omega_k^*(\rho, \theta) [E - H(q, \rho, \theta)] \Omega_{k'}(\rho, \theta) Q_{i'}(q) a_{i'k'} \right\}. \tag{18}$$

The quantity,

$$H(q, \rho, \theta) = -\frac{1}{2M}\left[\frac{\partial^2}{\partial q^2} + \frac{4}{q^2}\frac{\partial}{\partial \rho}(1 - \rho^2)\frac{\partial}{\partial \rho} + \frac{4}{q^2\rho^2}\frac{\partial^2}{\partial \theta^2}\right] + W(q, \rho, \theta) + \frac{15}{8Mq^2} \tag{19}$$

is the Hamiltonian of the system for the total angular momentum $J = 0$. Equation (18) uses the wave function expansion defined by Eq. (8).

We apply the p-version of the finite element method to express both $Q_i(q)$ and $\Omega_k(\rho, \theta)$. The procedure involves a basis function optimization for the hyperradius direction. First, we choose ρ and θ values such that the q-direction line passes through the potential energy surface minimum. The Hamiltonian, constrained to the one-dimensional degree of freedom, is diagonalized and the q-direction eigenfunctions are used as basis functions for expanding the full three-dimensional state. The p-version of the finite element is used to calculate the optimized basis

functions. The advantage of generating these functions numerically is that the procedure is quite general and works for any system.

We show the performance of the p-version of the finite element method for solving one-dimensional problems in Table 1. We use a Morse potential fitted to the H_2 molecule in order to have a neat idea of the convergence. As we can see, this method is able to converge all vibrational states of H_2 very accurately. We utilized 90 elements, with polynomials of up to the tenth degree in each element, and the inter nuclear distance was taken from 0 to 15 bohr.

The hyperangular (ρ, θ)-space is expressed by means of a two-dimensional finite element method expansion. We first optimized the mesh of triangles. We performed several tests and realized that a regular network is preferred to another conformation. The p-version of the finite element is then applied. We also noticed that the best strategy is a uniform distribution of polynomials over the whole space. The fact that highly excited vibrational eigenfunctions are spread over a large part of the hyperangular space explains why we need a regular network and a uniform distribution of polynomials.

The molecule under study has a permutation symmetry due to the presence of the two identical hydrogen atoms and we can use it to simplify the calculation. As we mentioned before, the hyperangles ρ and θ are defined in the ranges $\rho = [0, 1]$ and $\theta = [0, 2\pi]$. The potential energy surface of H_2O, written in hyperspherical coordinates, expresses its symmetry uniquely through the hyperangle θ. The potential has the same behavior for the hyperangle ranging from $\theta = 0 \rightarrow \pi$ and $\theta = \pi \rightarrow 2\pi$, therefore, the wave function must be even or odd when crossing the

Table 1. The performance of the one-dimensional finite element p-version. Comparison between the calculated eigenvalues of H_2 and the exact ones. We used the interval 0.0–15.0 discretized by 90 elements. The wave function was expanded by p-version functions up to the 10th degree. All values re expressed in cm^{-1}

State	Calculation	Exact
1	2166.1	2166.1
2	6308.9	6308.9
3	10199.4	10199.4
4	13837.6	13837.6
5	17223.4	17223.4
6	20356.9	20356.9
7	23238.0	23238.0
8	25866.8	25866.8
9	28243.3	28243.3
10	30367.4	30367.4
11	32239.2	32239.1
12	33858.6	33858.6
13	35225.7	35225.5
14	36340.4	35340.2
15	37202.7	37202.5
16	37812.9	37812.6
17	38170.6	38170.4

line that divides these two regions. In the following, we label each state using its symmetry.

The dimension of the matrix associated with the expansion defined by Eq. (8) is given by $I \times K$, where, I and K are the number of basis functions used for expanding the q and (ρ, θ) spaces, respectively. The finite element method usually produces large matrices, therefore K tends to be large and the final matrix, of dimension $I \times K$, will not be tractable. A truncation method should be designed. A procedure commonly used to deal with this problem has been proposed by Light and collaborators [1–6] and is known in the literature by the name of successive diagonalization and truncation technique.

The successive diagonalization and truncation technique is applied as follows. The (ρ, θ)-diagonal blocks, obtained when $i = i'$ in Eq. (18) are diagonalized and the (ρ, θ)-eigenvectors are used as optimized basis functions. The off-diagonal (ρ, θ)-blocks, defined when $i \neq i'$, are then built in terms of these new numerical basis functions. The number of basis functions to be retained is determined by a cut-off energy. Our computational resources allowed us to retain the (ρ, θ)-basis associated with eigenvalues up to 0.25 hartree above the minimum of the potential energy function.

5. Results

The program begins by optimizing the basis functions for the hyperradial direction. We found that for $\rho = -0.304$, $\theta = 0.0$ the q-direction line passes through the bottom of the potential. The potential energy surface behavior in the q-direction, for any bound triatomic system, is similar to a morse potential (see Ref. [53]). The hyperradius interval $0.0 \rightarrow 5.0$ bohr and 170 elements, with p-version polynomials up to $S_{10}(q)$ per element, has been used to calculate them. We needed 16 of these functions to calculate the vibrational states for H_2O showed in Table 2.

A previous calculation by Bačić et al. [14] utilized a Sorbie–Murrell-type potential energy surface. Their calculation is not in good agreement with the experimental data. We believe that the discrepancy is due to the potential energy surface since the authors used to procedure that has been applied to several other molecules and provided good results for them. The more recent calculations by Fernley et al. [18], Wei and Carrington [19] and Choi and Light [20] used Jensen's surface [17] and reproduced the experimental data well.

We used the same potential utilized by Miller and Tennyson [18], Wei and Carrington [19] and Choi and Light [20]. This is an empirical potential surface obtained by Jensen [17] who collected a large amount of experimental data to fit it. Table 2 shows states of the water molecule for the even symmetry up to $16000\,cm^{-1}$ and odd symmetry up to $13000\,cm^{-1}$. We also compare the calculated numbers with experimental values and calculations by Fernley et al. [18], Wei and Carrington [19] and Choi and Light [20] in this table and conclude that they are in good agreement. Many of the calculated numbers are less than $1\,cm^{-1}$ off from the experimental determination. Some states, however, show deviations higher than $10\,cm^{-2}$ from the experimental results and from the other calculations. There are three key parameters which can be responsible for such deviations: the number of q-basis functions, the number of finite elements describing the (ρ, θ)-space and the quantity of (ρ, θ)-basis functions. We did several tests including other finite element meshes and also varied the number of (ρ, θ)-basis functions and these

Table 2. Symmetric and anti symmetric vibrational states of H_2O. The values are expressed in cm^{-1}. The calculated zero point energy (ZPE) is 4629.978 cm^{-1}. The experimental values have been taken from Ref. [17]

State	WC[a]	FMT[b]	CL[c]	Present	Obs.
(010)	1594.3	1594.3	1594.3	1594.2	1594.7
(020)	3152.0	3152.0	3152.0	3152.0	3151.6
(100)	3656.4	3656.5	3656.4	3656.1	3657.0
(001)	3755.9	3756.0	3755.9	3755.7	3755.9
(030)	4667.7	4667.7	4667.6	4667.9	4666.8
(110)	5234.2	5234.3	5234.2	5233.9	5234.9
(011)	5332.0	5333.2	5332.0	5331.8	5331.2
(040)	6134.1	6134.2	6134.1	6134.9	6134.0
(120)	6775.0	6775.1	6775.0	6774.8	6775.0
(021)	6873.4	6873.5	6873.4	6873.5	6871.5
(200)	7202.6	7202.7	7202.6	7202.1	7201.5
(101)	7250.9	7251.0	7250.9	7250.4	7249.8
(002)	7444.9	7445.0	7444.9	7444.6	7445.0
(050)	7539.7	7539.0	7539.8	7541.4	?
(130)	8273.2	8273.3	8273.2	8273.2	8273.9
(031)	8375.6	8375.7	8375.6	8376.3	8373.8
(210)	8762.8	8763.0	8762.8	8762.3	8761.5
(111)	8809.5	8809.7	8809.5	8809.2	8807.0
(060)	8863.2	8863.3	8863.2	8865.9	?
(012)	9002.1	9002.2	9002.1	9001.8	9000.1
(140)	9719.7	9719.7	9719.7	9720.2	?
(041)	9832.5	9834.5	9832.5	9834.1	9833.6
(070)	10073.8	10073.9	10073.8	10078.0	?
(220)	10285.4	10285.9	10285.7	10286.9	10284.4
(121)	10332.4	10332.5	10332.4	10333.0	10328.7
(022)	10525.6	10525.7	10525.6	10530.9	10524.3
(300)	10602.7	10602.9	10602.7	10601.8	10599.6
(201)	10615.5	10615.7	10615.6	10612.9	10613.4
(102)	10869.3	10869.4	10869.3	10868.3	10868.8
(003)	10034.0	10034.2	10034.1	10033.5	10032.4
(150)	?	11082.4	11082.2	11084.8	?
(080)	?	11234.5	11234.3	11238.3	?
(051)	?	11235.3	11235.2	11242.1	?
(230)	?	11766.3	11766.2	11765.7	?
(131)	11815.4	11815.6	11815.4	11816.4	11813.2
(032)	?	12011.6	12011.5	12010.1	?
(310)	12144.4	12144.6	12144.4	12143.5	12139.2
(211)	12156.5	12156.7	12156.5	12156.8	12151.3
(160)	?	12340.8	12340.7	12353.6	?
(112)	12408.4	12408.6	12408.4	12407.5	12407.6
(090)	?	12504.2	12504.0	12516.4	?
(061)	?	12567.2	12567.0	12570.6	?
(013)	12567.0	12571.5	12571.3	12572.7	12565.0
(240)	?	13195.9	13195.8	13195.2	?
(141)	?	13252.7	13252.5	13253.7	?
(042)	?	13453.7	13453.6	13451.2	?
(170)	?	13604.9	13604.8	13616.7	?
(320)	?	13647.9	13647.7	13667.8	?
(221)	13647.7	13658.9	13658.7	13670.6	13652.7
(0100)	?	13793.5	13793.4	13824.1	?

Table 2. (Continued)

State	WC[a]	FMT[b]	CL[c]	Present	Obs.
(202)	13829.7	13829.9	13829.7	13827.2	13828.3
(122)	13911.7	13911.9	13911.7	13939.2	13910.8
(400)	14223.5	14223.7	14223.4	14217.7	14221.1
(004)	14541.3	14541.5	14541.3	14526.0	14536.8
(250)	?	14549.3	14549.2	14551.2	?
(180)	?	14778.4	14778.3	14788.8	?
(052)	?	14859.1	14858.9	14861.7	?
(330)	?	50109.8	15109.6	15101.6	15107
(0110)	?	15181.4	15181.4	15248.4	?
(212)	15350.1	15350.3	15350.1	15344.8	15344.4
(132)	?	15377.2	15377.0	15365.6	?
(410)	15744.1	15744.3	15744.0	15736.6	15742.7
(260)	?	15809.4	15809.3	15819.7	?
(190)	?	16023.8	16023.7	16031.6	?
(014)	?	16057.8	16057.6	16040.8	?
(062)	?	16187.2	16187.0	16194.4	?

[a] Wei and Carrington [19]
[b] Fernley et al. [18]
[c] Choi and Light [20]

Table 3. Parameters and conversion factors utilized in the calculation

Hydrogen mass	1837.416951 au
Oxygen mass	29156.946713 au
Hyperradius range	0.0 to 5.0 bohr
Number of elements used for optimizing the hyperradial functions	170
Number of optimized hyperradial functions	16
Number of triangles used to determine the (ρ, θ)-functions	841
Cut-off energy used for keeping the (ρ, θ)-functions	0.25 hartree (above the minimum of the potential energy surface
Conversion factor between hartree and cm^{-1}	1 hartree = 219474.6 cm^{-1}

levels did not change significantly. Unfortunately, it was impossible to increase the number of q-basis as we were at the limit of memory of our machine.

A mesh of 841 triangles has been used and that produced finite element method matrices of dimension 1395 to be diagonalized. The eigenvectors of these matrices were used as the (ρ, θ)-basis functions. We stress that the finite element method matrices are symmetric and sparse. The final contracted matrix had the dimension 599×599 for the even symmetry and 558×558 for the odd one. The program took 6–7 h of CPU of a VAX-8350 to run each symmetry.

Finally, in Table 3, we give all parameters and conversion unit factors we applied in this calculation. The hyperradial range from 0 to 5 bohr used here has been determined by means of several test runs. The energy cut-off utilized for keeping the (ρ, θ)-eigenfunctions was 0.25 hartree above the minimum of the

potential energy surface. All calculations have been done in atomic units and the final energies converted to cm^{-1}.

6. Conclusions

The p-version of the finite element method provided a stable and reliable algorithm to calculate bound states of triatomic molecules and the fully three-dimensional wave function was obtained. Moreover, the symmetry associated with the problem was easily implemented. The method was applied to the calculation of the bound states of the water molecule and converged many levels for both even and odd symmetries. In this way, we showed that the finite element method can be used to calculate highly excited vibrational states of triatomic systems. We also point out that the procedure is quite general and may readily be applied to other molecules. The algorithm involves the optimization of functions for both the hyperradial direction and the hyperangular space and uses the p-version of the finite element method to perform such optimizations. The final contracted matrix had the dimension 599×599 for the even symmetry and 558×558 for the odd one.

Acknowledgements. We dedicate this paper to Professor Jan Linderberg who has introduced one of us (JJSN) into this field. We take the opportunity to express our admiration for Prof. Linderberg's scientific work and congratulate him on his 60th birthday.

This work was supported by "Conselho Nacional de Desenvolvimento Científico e Tecnológico" (CNPq) through grants to J. J. Soares Neto and F. V. Prudente. The computer facilities were provided by the "Laboratório de Cálculo Cientifico" at Department of Physics, University of Brasilia. Professors J. D. Mangueira Vianna, N. S. Correia and T. M. da Rocha Filho read the manuscript and gave interesting suggestions. We thank Amy Shaw for giving several suggestions concerning the style and grammar.

References

1. Bačić Z, Light JC (1986) J Chem Phys 85:4594
2. Bačić Z, Whitnell RM, Brown D, Light JC (1988) Comp Phys Comm 51:35
3. Bačić Z, Light JC (1987) J Chem Phys 86:3065
4. Light JC, Bačić Z, J Chem Phys (1987) 87:4008
5. Mladenovic M, Bačić Z (1990) J Chem Phys 93:3039
6. Bentley JA, Bowman JM, Gazdy B, Lee TJ, Dateo CE (1992) Chem Phys Lett 198:563
7. Choi Seung E, Light JC, J Chem Phys (1990) 92:2129
8. Tennyson J, Sutcliffe BT (1984) Mol Phys 51:887
9. Tennyson J, Sutcliffe BT (1986) Mol Phys 58:1067
10. Henderson JR, Tennyson J (1990) Chem Phys Lett 173:133
11. Carter S, Meyer W (1990) J Chem Phys 93:8902
12. Bačić Z, Zhang JZ (1991) Chem Phys Lett 184:513
13. Bačić Z, Zhang JZ (1992) J Chem Phys 96:3707
14. Bačić Z, Watt D, Light JC (1988) J Chem Phys 89:947
15. Sorbie KS, Murrel JN (1975) Mol Phys 29:1387
16. Soares Neto JJ, Linderberg J (1991) J Comp Chem 12:1237
17. Jensen P (1989) J Mol Spectrosc 133:438
18. Fernley JA, Miller S, Tennyson J (1991) J Mol Spectrosc 150:597
19. Wei H, Carrington T (1992) J Chem Phys 97:3029
20. Choi SE, Light JC (1992) J Chem Phys 97:7031
21. Tennyson J (1993) J Chem Phys 98:9658

22. Allen HC (1963) Molecular Vib-rotors: The theory and interpretation of high resolution infrared spectra, Wiley, New York
23. Linderberg J, Padkjær SB, Öhrn Y, Vessal B (1989) J Chem Phys 90:6254
24. Pack RT, Parker GA (1987) J Chem Phys 87:3888
25. Launay JM, Le Dourneuf M (1989) Chem Phys Lett 163:178
26. Launay JM, Le Dourneuf M (1990) Chem Phys Lett 169:473
27. Le Quéré F, Leforestier C (1991) J Chem Phys 94:1118
28. Soares JJ, Padkjær SB, Linderberg J (1989) Int J Quantum Chem S23:127
29. Soares Neto JJ, Linderberg J (1991) Comp Phys Comm 66:55
30. Whitnell RM, Light JC (1989) J Chem Phys 90:1774
31. Mead CA (1980) J Chem Phys 72:3839
32. Linderberg J (1987) Comp Phys Rep 6:209
33. Linderberg J, Vessal B (1987) Int J Quantum Chem 31:65
34. Mishra M, Linderberg J, Öhrn Y (1984) Chem Phys Lett 111:439
35. Soares Neto JJ, Linderberg J (1991) J Chem Phys 95:8022
36. Ciarlet PG (1978) The finite element method for elliptic problem, North-Holland, Amsterdam
37. Norrie DH, de Vries G (1973) The finite element method, Academic Press, New York
38. Morton KW (1987) Comp Phys Rep 6:1
39. Clementi E, Chakravorty SJ, Corongi G, Sonnad V (1990) in: Clementi E (ed) MOTEC-Modern techniques in computational chemistry, 47
40. Soares Neto JJ, A parallel algorithm for calculating ro-vibrational states of diatomic molecules, to be published in J Comp Chem
41. Gronwall TH (1937) Phys Rev 51:665
42. Bartlet Jr. JH Phys Rev (1937) 51:661
43. Smith FT (1960) Phys Rev 120:1058
44. Smith FT (1962) J Math Phys 3:735
45. Kuppermann A (1975) Chem Phys Lett 32:374
46. Johnson BR (1980) J Chem Phys 73:5051
47. Johnson BR (1983) J Chem Phys 79:1906
48. Jaquet R (1987) Theor Chim Acta 71:425
49. Jaquet R (1987) Chem Phys 118:17
50. Sato N, Iwata S (1988) J Comp Chem 9:222
51. Kuppermann A, Hipes PG (1986) J Chem Phys 84:5963
52. Parker GA, Pack RT, Laganà A, Archer BJ, Kress J, Bačić Z (1989) in: Laganà A (ed), Super computer algorithms for reactivity, dynamics and kinetics of small molecules, Reidel, Dordrecht
53. Padkjær SB, Soares JJ, Linderberg J (1992) Chem Phys 161:419
54. Soares JJ, Padkjær SB, Linderberg J (1990) Int J Quantum Chem S24:467
55. Linderberg J, Öhrn Y, Padkjær SB (1989) J Chem Phys 91:4793
56. Levin FS, Shertzer J (1985) Phys Rev A32:3285
57. Levin FS, Shertzer J (1988) Phys Rev Lett 61:1089
58. Schulze W, Kolb D (1985) Chem Phys Lett 122:271
59. Yang L, Heinemann D, Kolb D (1992) Chem Phys Lett 192:499
60. Flores JR, Clementi E, Sonnad V (1989) J Chem Phys 91:7030